

# Design and Fabrication of a Microelectromechanical Relay

by  
Hans-Georg Liemke

Submitted to the Department of Mechanical Engineering  
in partial fulfillment of the requirements for the degree of  
Bachelor of Science in Mechanical Engineering  
at the  
MASSACHUSETTS INSTITUTE OF TECHNOLOGY  
May 1994

© Massachusetts Institute of Technology 1994. All rights reserved.

Author.....  
Department of Mechanical Engineering  
May 9, 1994

Certified by.....  
Jeffrey H. Lang  
Professor, Electrical Engineering and Computer Science  
Thesis Supervisor

Certified by.....  
Martin A. Schmidt  
Associate Professor, Electrical Engineering and Computer Science  
Thesis Supervisor

Accepted by.....  
Peter Griffith  
Chairman, Departmental Committee on Undergraduate Students

ARCHIVES

MASSACHUSETTS INSTITUTE  
OF TECHNOLOGY

JUL 13 1994

# **Design and Fabrication of a Micro Electromechanical Relay**

by

Hans-Georg Liemke

Submitted to the Department of Mechanical Engineering on May 11, 1994 in partial fulfillment of the requirements for the Degree of Bachelor of Science in Mechanical Engineering

## **Abstract**

This thesis describes the design and fabrication of a micro electromechanical relay. Micro fabrication offers the opportunity to reduce the feature size of conventional relays and also enhances some of their performance parameters such as switching time, fatigue properties, and breakdown voltage.

Our relay design consists of two bonded wafers. One wafer has a mechanical spring structure etched in a 5  $\mu\text{m}$  thick layer of doped bulk silicon. Metal is deposited on the base of the spring structure as contact metal. The second wafer features two trenches that house the metal for an electrostatic actuator and for the second electrical contact. The actuation metal and the spring structure form a parallel plate capacitor. A voltage applied to the actuation metal will pull down the spring structure down and close the electrical contact.

The fabrication process uses a KOH etch up to a heavily boron doped etch stop to produce thin membranes. These membranes are then plasma etched to release the spring structure. The trenches on the second wafer are produced with a timed KOH etch.

We present a mechanical design that considers the problems associated with micro fabrication. The spring structure is designed such that residual stresses in the doped silicon layer are relieved. Furthermore, the area that has to be removed during the plasma etch is minimized. Additionally, we provide springs in three different sizes to test a range of actuation voltages.

An overview of the processing sequence of this device, including the fabrication of the two wafers, the metallization and the bonding process, is discussed and photographs of the spring and the metal trenches are shown.

During the initial testing of the prototypes we observed that most relay springs were either initially touching the actuation metal or got stuck after the first visible pull down. Some devices showed continuous operation, but we were unable to determine whether an electrical contact was achieved.

Thesis Supervisor: Martin A. Schmidt

Title: Associate Professor, Electrical Engineering and Computer Science

Thesis Supervisor: Jeffrey H. Lang

Title: Professor, Electrical Engineering and Computer Science

## **Acknowledgments**

I would like to thank Professor Martin Schmidt and Professor Jeffrey Lang for giving me the opportunity to take on this exiting project. They provided me with the necessary knowledge and enthusiasm to enter the field of micro machining.

Special thanks are deserved by the students in the 6.151J/3.156J project laboratory who made the fabrication of the prototypes possible. Without them I would have not been able to produce working devices in such a short time. For that important part, I thank the entire class, namely, Remzi Dokmeci, Laura Juliano, Mattan Kamon, Yolanda Leung, Barbara Nichols, and Testuo Ohara.

I also thank May Lu who invested a lot of time to assist me in the design of the relay and help us all with the fabrication of the device. Her skill and commitment were essential for the success of this project.

# Contents

<b>1. Introduction</b> .....	<b>6</b>
1.1 Motivation .....	6
1.2. Thesis Overview .....	7
<b>2. Design</b> .....	<b>9</b>
2.1 Design Overview .....	9
2.2. Design Details .....	17
2.3. Mask Layout.....	22
<b>3. Fabrication</b> .....	<b>33</b>
3.1. Overview .....	33
3.2. Spring Wafer .....	33
3.3. Handle Wafer .....	37
3.4 Metallization .....	39
3.5 Bonding and Alignment.....	40
<b>4. Results</b> .....	<b>43</b>
4.1 Fabrication Results .....	43
4.2 Experimental Testing Results .....	44
<b>5. Conclusion</b> .....	<b>46</b>
<b>Appendix A</b> .....	<b>50</b>

# 1. Introduction

## 1.1 Motivation

The simple mechanical design of a relay switch offers the opportunity to implement this device on a silicon wafer using micro fabrication techniques. We hope that this enables us to reduce the feature size of relays below  $1 \text{ mm}^2$ . The use of silicon processing technology also allows us to fabricate a micro mechanical relay on the same chip as associated electronics, further reducing the packaging density of such hybrid devices. Combined fabrication can significantly reduce the size of power electronics that previously used conventional relays. In comparison to conventional relays micro relays not only offer a smaller feature size, but also a reduced switching time and the good fatigue properties of silicon. Additionally, micro relays feature a lower on resistance and a higher breakdown voltage than power transistors making them an attractive device in a wide range of applications.

A potential market for micro relays is the automotive industry which still uses conventional relays. The mentioned advantages of micro relays justify the use in the mass production of cars if their installation becomes economically feasible. In order to become an attractive part for the automotive industry the unit price of micro relays must in the range of \$5 (which is close to the price of conventional relays). Fortunately, semiconductor processing technology allows us to mass produce the device at a low price. Large semiconductor companies are the ideal manufacturers for this product and should be capable of producing it at a low unit price.

Another potential application is a matrix switch as proposed by NTT [1]. Arrays of relays and related control electronics that are fabricated on the same

wafer are particularly useful in telecommunication, since this application requires high speed switching but not large contact cycles or large electrical loads. Micro relays are ideal for high speed switching operations since we expect cycle times of more than 1 kHz.

In addition to these concrete examples there exist more conceptual applications of our design. Since the mechanical part of the micro relay is essentially a small linear actuator, many other devices or machines that are similar to the relay and use the same mechanism are possible. The actuator could ultimately be used to transmit a small force in larger Micro Electromechanical Systems (MEMS).

## **1.2. Thesis Overview**

This thesis discusses the design and fabrication of a micro electromechanical relay. We also include test results of several prototypes that are fabricated as part of the 6.151J semiconductor project laboratory.

In the section on the design of the relay we describe the various design stages that preceded the layout of the mask set for the fabrication process. First, several design options for the production of a micro mechanical relay are described. After a careful evaluation of these options we select a final design approach and specify its details.

Our proposed relay consists of two bonded wafers. Figure 1.2 shows an exploded view of the design. The top wafer, referred to as the "spring wafer" has a mechanical spring structure etched in a 5  $\mu\text{m}$  thick layer of doped bulk silicon. Metal is deposited on the base of the spring structure as contact metal. Located next to the spring structure are two contact holes that are etched through the entire wafer and establish access to the bottom wafer. This wafer is referred to as

the “handle wafer” and has two trenches that house metal for an electrostatic actuator and for the second electrical contact. The actuation metal and the  $p^{++}$  doped spring structure form a parallel plate capacitor. A voltage applied to the actuation metal will pull down the spring structure and close the electrical contact.

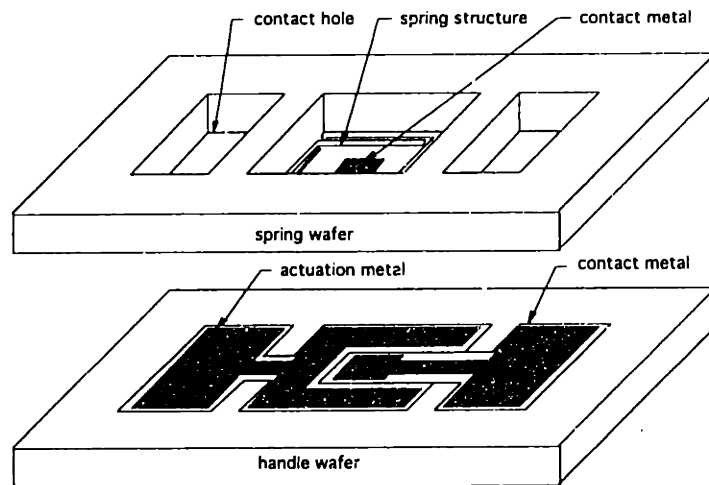


**Figure 1.2:** Exploded View of the Micro Relay

We then describe how we initially sized the spring structure and the area of the actuation metals. In the section on the design details we perform calculations based on these initial results and specify the exact sizes for the mechanical structure and actuation. Since many of the material properties of silicon cannot be predicted before the fabrication process we offer a range of stiffness for the spring and intend to build the relay in three different sizes. For each size the corresponding spring constant and the actuation voltage are calculated.

In the following subsection on mask design we continue to describe the mask design for the silicon fabrication process. In addition to a standard relay structure, a 4-point probe is included in the mask set to provide a platform for contact resistance measurements of different contact metals. We also describe the

test structures that we use to monitor the fabrication and to test the mechanical properties of the silicon.

In the chapter on the fabrication of the device we describe the process modules that were developed by four different groups of students as part of the 6.151J project lab. The groups worked on the fabrication of the spring wafer, the handle wafer, the metallization, and the alignment and bonding of the device.

We conclude this report with the results of the experimental test of several prototype relays and recommend future improvements for the fabrication of a micro relay.

## **2. Design**

### **2.1 Design Overview**

Micro machining technology provides several options for the actuation mechanisms of micro mechanical relays. As we evaluate these options we must be concerned about the switching time, actuation force, reliability, and fabrication process of each individual idea. It is also important that we consider whether the device can be manufactured with our available laboratory facilities, since we intend to produce working prototypes of our design.

One of the design options is a relay with thermo pneumatic actuation. Figure 2.1.1 shows a cross-section of this approach. Here, a gas is enclosed in a sealed cavity and heated by an electrical resistor. As the pressure in the cavity increases it deflects a thin silicon membrane. The deflection of the membrane is used to open and close the switch contact. A significant disadvantage of this idea is the complicated fabrication process. It is necessary to bond three silicon wafers to build a cavity and a switching mechanism. Another problem is the complicated



access to the contact metals and to the embedded heating resistor. Both elements would have to be contacted through the backside of the wafer. Limited heat transfer to the gas in the cavity also negatively influences the cycle time of this device. We expect a very low switching frequency for this relay and assume that a fast actuation time requires a large power consumption of the heating resistor.

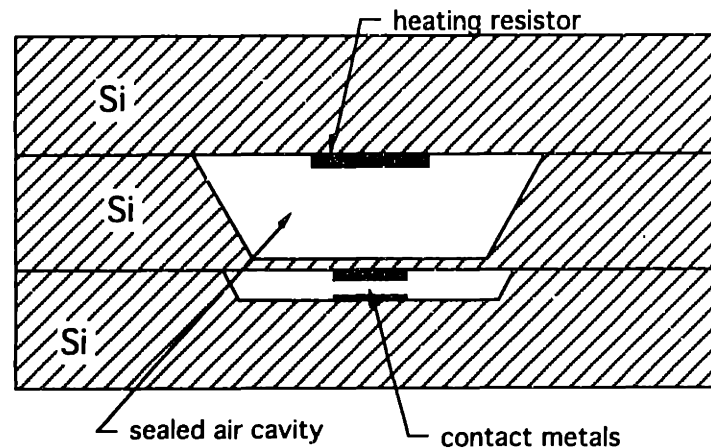


**Figure 2.1.1:** Thermo Pneumatic Relay

A second switching mechanism is a bimetallic strip deposited on a thin silicon membrane as shown in Figure 2.1.2. If the strip is heated, the different thermal expansion coefficients of the two metals cause the strip to bend and the membrane to deform. If the membrane deforms uniformly and linearly, it can be used to actuate a switch contact. Problems that might constraint the use of this method are the deposition of a functional bimetallic strip and the slow actuation time of the membrane due to the limited heat transfer.

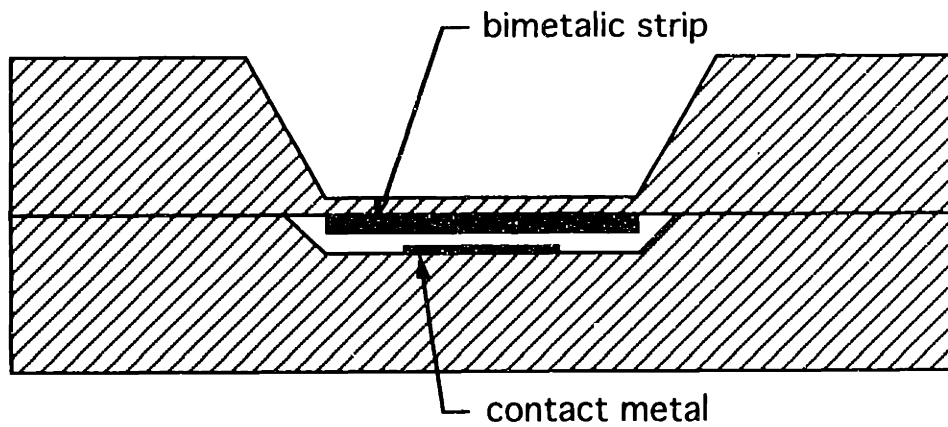


**Figure 2.1.2: Bimetallic Relay**

A third option is the fabrication of a silicon spring structure that is actuated by an electrostatic capacitor. The parallel plate capacitor is formed by two bonded wafers. One plate is the heavily  $p^{++}$  doped base plate of a spring structure that is etched in a thin layer of bulk silicon. The second plate of the capacitor is metal deposited on the handle wafer. An exploded view and a cross section of this idea are shown in Figure 1.2 and Figure 2.1.3. The speed of this relay is much faster than that of the two previous relays due to the fast charging rate of the capacitor, and it can also be fabricated with our available laboratory equipment.

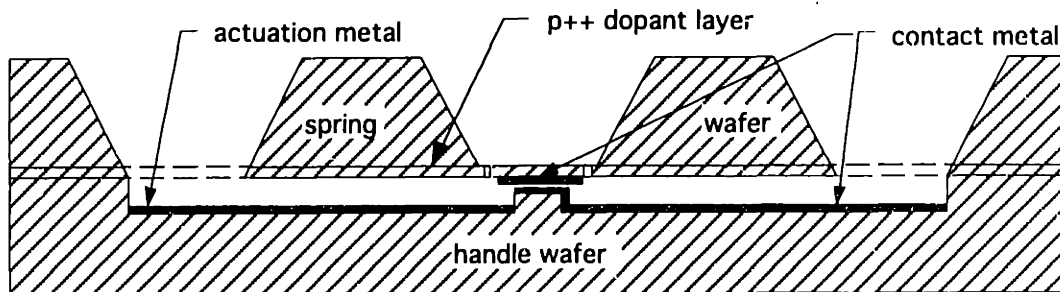


**Figure 2.1.3: Silicon Spring Relay**

Contact metal is deposited on the base plate of the spring structure and on the section of the handle wafer that is touching the spring wafer. The handle wafer is fabricated with two etched trenches that house the contact and the actuation metal. The contact metal on the handle wafer is deposited on a square pedestal formed by the two trench etches. At this point the contact metal is 5  $\mu\text{m}$  above the actuation metal. After the bonding process the gap size between the two contact metals is approximately 5  $\mu\text{m}$  and the gap size between the actuation metal and the spring structure is 10  $\mu\text{m}$ . The step ensures that the actuation metal does not touch the spring wafer during the contact. To access the metal on the handle wafer, large contact holes are etched in the spring wafer. For the operation of the prototype switches three electrical connections must be made. For the actuation and one switch contact, two probes must touch the metal pads on the handle wafer. The other switch contact is established at the silicon surface on the backside of the spring wafer. Here, the conductive path between the contact metal and the contact probe is going through the heavy  $p^{++}$  doped layer and the  $p^+$  bulk silicon of the spring wafer rather than only through metal. Consequently, we expect a higher resistance than at the other contact points.

Our main concern during the design of the micro relay is the realization of a functional spring structure. The spring must displace vertically and must be able to deflect more than 5  $\mu\text{m}$ . The displacement should also be fairly linear and the stiffness should be large enough to provide a restoring force that returns the metal contacts to their original position once the actuation voltage is turned off. The linear vertical displacement requires a symmetrical spring structure that restricts lateral motion. A simple approach is a square base plate supported by four cantilevers. If the base plate is displaced to close the switch, the four

cantilevers bend. The stiffness of the silicon cantilevers provides the restoring force for the spring.

The spacing between the electrical contact plates and therefore the required spring deflection can be adjusted during the processing of the wafers by alternating the depth of the trenches on the handle wafer or by adjusting the thickness of the bonding material. It is also assumed that the thickness of the spring membrane due to processing restrictions and the minimum required stability of the structure is not smaller than  $5\ \mu\text{m}$ . Additionally, it is important to recognize that silicon is a brittle material that fails at strains of more than 1%. The design should have a safety factor of 10 to allow unpredictable stresses during the processing of the wafer and large residual stresses. Consequently, the maximum strain should not exceed 0.1%.

One of the simplest designs for the spring structure is a square base area that is supported by four straight tethers (see Figure 2.1.4).

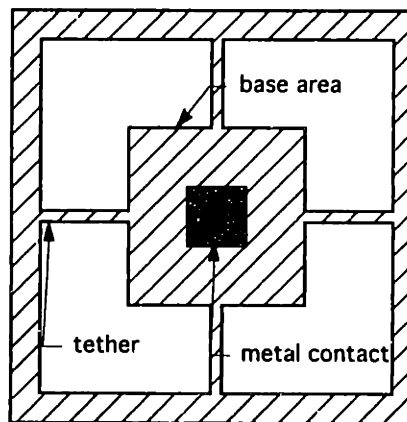


**Figure 2.1.4: Base Plate with Straight Tethers**

If the contact area is displaced vertically, each tether experiences a bending force. Because of the symmetry of the structure the angle of deflection at both ends of the tether is zero (see Figure 2.1.5).

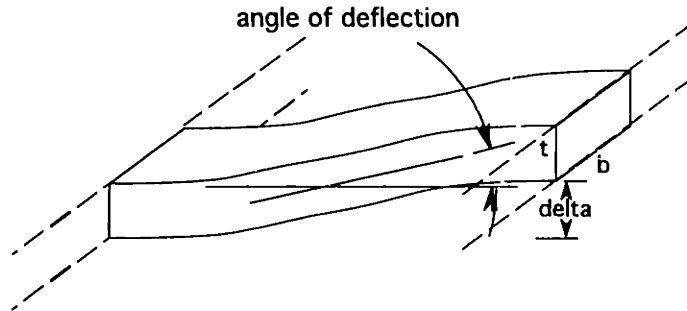


**Figure 2.1.5: Deflection of Cantilevers**

If four tethers are used, the deflection  $\delta$  of the base area is related to the force  $F$  by the following equation [2]:

$$\delta = \frac{Fl^3}{4Ebt^3}. \quad (2.1.1)$$

$E$  is the Young's modulus of silicon,  $b$  the width of tether, and  $t$  is its thickness.

The maximum bending strain in the beam is described by the equation:

$$\varepsilon = \frac{\sigma}{E} = \frac{F l t}{4} \frac{12}{2 E b t^3} = \frac{3Fl}{4Ebt^2}. \quad (2.1.2)$$

Combining these two equations, assuming a deflection  $\delta$  of  $5 \mu\text{m}$ , a thickness  $t$  of  $5 \mu\text{m}$ , and a width  $b$  of  $50 \mu\text{m}$ , it follows that a beam length of at least  $280 \mu\text{m}$  is required to keep the maximum strain below  $0.1 \%$ . Any longer tether structure experiences less strain at a given deflection.

To reduce the size of the spring and minimize the width of the etched trenches it is preferred to position the beams parallel to the sides of the base area (see Figure 2.1.6). This design also relieves residual stress in the material. Now the length of the beams determines the size of the base area.

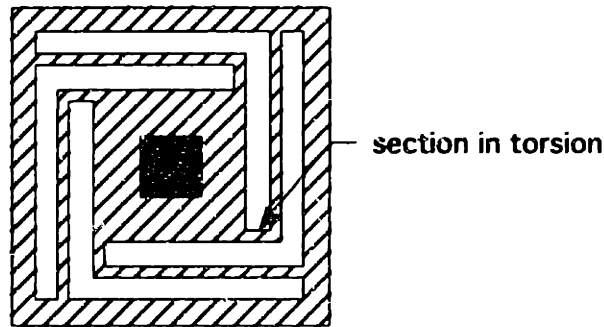


**Figure 2.1.6: Base Plate with Parallel Tethers**

Since the alignment error for the wafer bonding process is about  $50\ \mu\text{m}$ , it is necessary to scale one metal contact larger than the other contact area to guarantee a full contact during operation (see Figure 2.1.7). A  $500\ \mu\text{m} \times 500\ \mu\text{m}$  base area will be sufficient to compensate the alignment error, maintain a large contact area of  $200\ \mu\text{m}$  side length, and still have a large enough area for the electrostatic actuator.

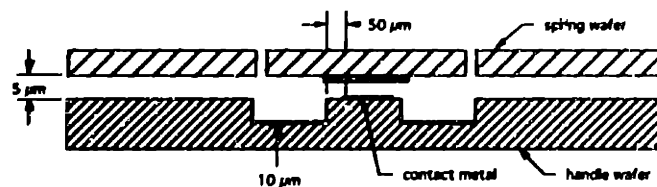


**Figure 2.1.7: Alignment Error**

The force required to deflect, by 5  $\mu\text{m}$ , a 600  $\mu\text{m}$  X 50  $\mu\text{m}$  X 5  $\mu\text{m}$  beam can be calculated from Equation 2.1.1 and is approximately 60  $\mu\text{N}$ . Since a small section of the beam is in torsion (see Figure 2.1.6), the shear strain due to torsion must be taken into consideration.

The maximum torsional shear stress  $\tau_{max}$  in a beam with rectangular cross section is given by the equation:

$$\tau_{max} = c_1 \frac{M}{ab^2}. \quad (2.1.3)$$

The variables  $a$  and  $b$  are the sides of the rectangular beam cross section, with  $a$  being the length of the longer side. The constant  $c_1$  depends on the ratio of  $a$  to  $b$ .  $M$  is the twisting moment acting on the beam.

The shear strain  $\gamma$  can be calculated with the formula:

$$\gamma = \frac{\tau}{G}. \quad (2.1.4)$$

The shear modulus  $G$  is estimated to be around  $1/2 E = 55 \text{ GN/m}^2$  [3]. To keep the shear stress below 0.1 % a beam width of more than 50  $\mu\text{m}$  is required at the section that is in torsion. The addition of this small section to the beam does not influence the previous bending calculations because of its small contribution to the overall length of the structure.

During the operation of the relay it is important that the electric field in the capacitor between the two bonded wafers does not exceed the break down field of approximately  $1.7 \times 10^8 \text{ V/m}$ . The force required for a deflection of 5  $\mu\text{m}$  is  $6.0 \times 10^{-5} \text{ N}$ . The effective area of the capacitor is (500  $\mu\text{m}$  X 500  $\mu\text{m}$ )-(200  $\mu\text{m}$  X

200  $\mu\text{m}$ ) =  $2.1 \times 10^{-7} \text{ m}^2$ . The electrostatic pressure  $P_{electric}$  to actuate the relay and the electric field  $E$  can be calculated as:

$$P_{electric} = \frac{1}{2} \epsilon_0 E^2 = 286 \text{ N / m}$$

$$E = \sqrt{\frac{572 \text{ Pa}}{\epsilon_0}} \approx 8 \times 10^6 \text{ V / m} \quad (2.1.5)$$

The electric field is about one order of magnitude smaller than the break down field. At a maximum gap between the two capacitor plates of  $d = 10 \mu\text{m}$  this corresponds to a voltage of  $U = E \times d \approx 100 \text{ V}$ .

This approach is not very accurate, but it can give us a rough estimate of the actuation voltages that we expect for the micro relay. A more accurate approach to calculate the actuation voltage is described in the next chapter.

## 2.2. Design Details

We base the more detailed calculations of the spring structure on a spring with a 500  $\mu\text{m}$  long base plate. We intend to release the spring structure with a plasma etch. The plasma etch must remove a 5  $\mu\text{m}$  thin layer of  $\text{p}^{++}$  doped silicon. The heavy doping of the silicon provides an etch stop for the KOH etch that produces the 5  $\mu\text{m}$  membranes. During the controlled plasma etch the lateral etch error can result in over- or under etching of up to 7  $\mu\text{m}$ . Having a trench of more than 20  $\mu\text{m}$  will ensure a complete release of the structure during this process. To increase the yield of the etch process we choose to have 30  $\mu\text{m}$  trenches and 50  $\mu\text{m}$  wide beams. This results in a maximum trench width of 37  $\mu\text{m}$  and a maximum beam width of 57  $\mu\text{m}$ . Knowing these parameters we calculate a beam length  $l$  of 610  $\mu\text{m}$  for a base plate with 500  $\mu\text{m}$  side length (see Figure 2.2.1). The



length of the section that is in torsion  $L_t$  is equal to the width of the plasma trench and equals  $30\ \mu\text{m}$ .

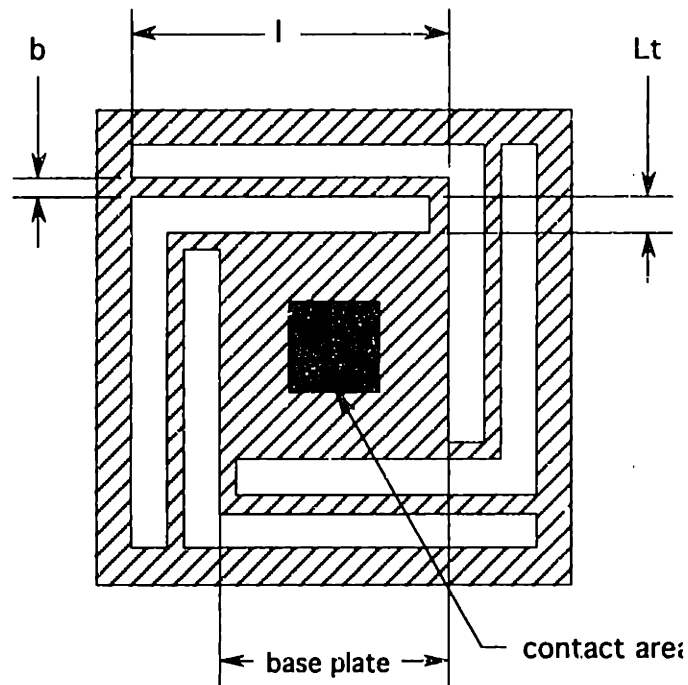


**Figure 2.2.1: Spring Structure**

Unfortunately, the heavy boron doping in the etch stop causes large residual stresses in the thin silicon membrane. According to the literature [2] stresses of up to  $30\ \text{MN}/\text{m}^2$  can occur in the doped region. It is important that the Boron concentration varies across thickness of the  $5\ \mu\text{m}$  membrane with a Gaussian distribution, the maximum being at the surface of the wafer. Consequently there is also a difference in residual stresses across the thickness of the membrane which causes it to deform.

However, it is very difficult and not within the range of this thesis to predict the stresses analytically. Instead we build the spring structure in three different sizes to have range of spring stiffness. If one structure deforms and we are not able to actuate the switch because it is too stiff or because both contact metals are

already touching, there is always the possibility that a larger or smaller structure will function.

Due to limitations during fabrication we set the minimum spring size to a base plate of 500  $\mu\text{m}$  side length. The other two sizes are 150 % and 200 % of this smallest size. Table 2.2.1 shows a summary of the dimensions of the three spring structures.

	Size 1	Size 2	Size 3
<i>base plate</i>	500 $\mu\text{m}$	750 $\mu\text{m}$	1000 $\mu\text{m}$
<i>l</i>	610 $\mu\text{m}$	910 $\mu\text{m}$	1220 $\mu\text{m}$
<i>b</i>	50 $\mu\text{m}$	70 $\mu\text{m}$	100 $\mu\text{m}$
<i>L<sub>t</sub></i>	30 $\mu\text{m}$	40 $\mu\text{m}$	60 $\mu\text{m}$

**Table 2.2.1: Spring Dimensions**

To calculate the exact force that is required to actuate the switch we consider the deflection due to the bending of the beam and due to the torsion.

The deflection  $\delta_b$  due to the bending is described by Equations 2.1.1 and 2.2.1:

$$\delta_b = \frac{F l^3}{4 E b t^3}, \quad (2.2.1)$$

where  $F$  is the force required to actuate the switch,  $l$  is the length of the beam,  $E$  is the Young's modulus of silicon,  $b$  is the width of the beam, and  $t$  is its

thickness. The deflection due to the torsion of the small section of the tether is defined by:

$$\delta_t = \varphi l = \frac{M_t L_t}{4Gc_2 b t^3} = \frac{F L_t}{2E c_2 b t^3}, \quad (2.2.2)$$

$\varphi$  is the angle of deflection,  $M_t$  is the moment that acts on the section that is in torsion,  $L_t$  is the length of the section in torsion, and  $c_2$  is a constant that depends on the ratio  $b/t$ .

The overall deflection is the sum of the deflections due to the beam bending and the torsion:

$$\delta = \delta_b + \delta_t. \quad (2.2.3)$$

However, we are interested in the force that is required to deflect the spring structure  $5 \mu\text{m}$ . Accordingly, Equation 2.2.2 is solved for the force  $F$  :

$$F = \frac{5 \mu\text{m}}{\left( \frac{l^2 L_t}{2E c_2 b t^3} + \frac{l^3}{4E b t^3} \right)} = Kd, \quad (2.2.4)$$

where  $K$  is the effective spring constant for the spring structure.

To calculate the minimum voltage that is required to actuate the relay structure the electrostatic force is set equal to the restoring force of the spring (see Figure 2.2.2 for details).

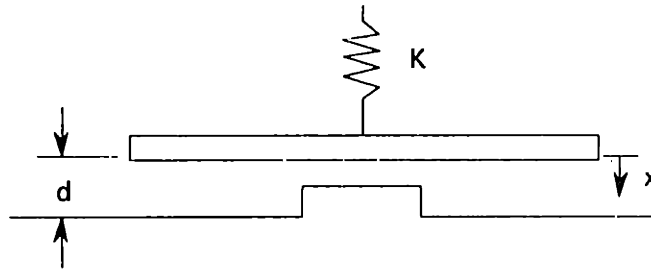


**Figure 2.2.2: Spring Deflection**

Thus,

$$Kx = \frac{1}{2} \epsilon_0 A \frac{V^2}{(d-x)^2}, \quad (2.2.5)$$

where  $x$  is the displacement of the spring,  $K$  is the spring constant,  $A$  is the area of the electrostatic actuator and  $V$  is the voltage applied between the spring and the actuation metal. The spring force and the electrostatic force reach a critical equilibrium when:

$$x = \frac{2}{3}d. \quad (2.2.6)$$

If we substitute this result in Equation 2.2.5, we calculate the minimum actuation voltage  $V_a$  to be:

$$V_a = \frac{2}{3} \sqrt{\frac{Kd^3}{3\epsilon_0 A}}. \quad (2.2.7)$$

The results for the various spring sizes are summarized in Tables 2.2.2 and 2.2.3.

	Size 1	Size 2	Size 3
$K$	9.09 N/m	4.00 N/m	2.38 N/m
$V_a$	33.94 V	22.52 V	8.77 V

**Table 2.2.2: Actuation Parameters for Standard Relay**

	Size 1	Size 2	Size 3
$K$	9.09 N/m	4.00 N/m	2.38 N/m
$V_a$	38.69 V	15.50 V	9.99 V

**Table 2.2.3: Actuation Parameters for 4-Point Probe**

We also check whether the weight of the spring base including the contact metal will cause a large deflection of the structure. We must consider the weight of the bulk silicon as well as the weight of the contact metal. Using conservative approximations we calculated a force of up to  $1 \times 10^{-7}$  N. This is two orders of magnitude smaller than the electrostatic forces that pull down the spring and can therefore be neglected.

### 2.3. Mask Layout

This is an experimental project and we do not intend to produce a micro relay at the smallest possible feature size. On the other hand we are concerned about the

dicing of this device, the handling of the wafer, large contact holes for easy access with a probe station and a reasonable high number of devices on a 2 inch wafer. Considering these issues we choose to have all structures sized at 5 mm X 10 mm. This size allows easy positioning in the dicing saw and is small enough such that we can arrange all structures on the wafer utilizing a large area of the wafer.

The standard relay has the spring structure positioned in the middle of the die and the contact holes on each side. The actuation metal itself is U-shaped and encloses the contact metal as shown in Figure 2.3.1. A 50  $\mu\text{m}$  metal strip leads to the contact holes which have a size of 1 mm X 1 mm. The KOH trenches for the contact holes and the spring structure are arranged in a line to facilitate probe access and to minimize the size of the overall structure.

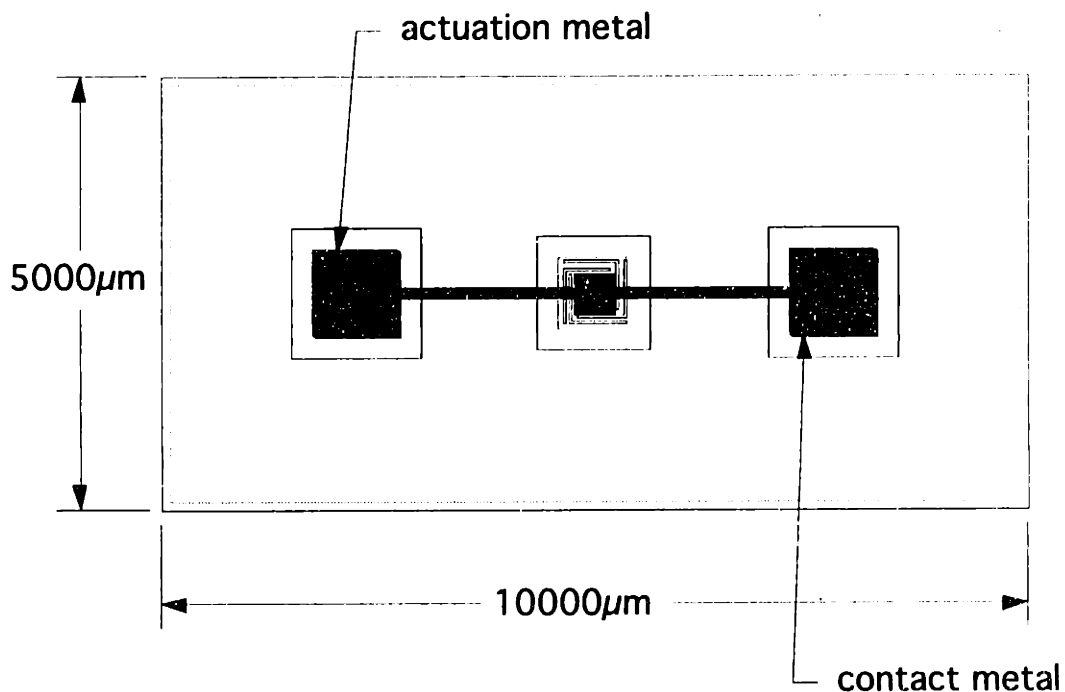


**Figure 2.3.1: Top View of the Standard Relay Die**

The arrangement of the 4-point probe is similar to the standard relay. Here, we have 6 KOH trenches arranged in a rectangle: one for the spring structure, one for the actuation metal, and four contact measurement points. The sizes of the spring structure for the 4-point probe are the same as the standard relay, but the shape of the actuation metal is different and consequently we expect different actuation voltages than for the standard relay (see tables 2.2.2 and 2.2.3). The actuation metal for the 4-point probe is H-shaped and more symmetrical than the actuation metal for the standard relay. The metal contact on the spring wafer touches two metal contacts on the handle wafer. Those two contacts are enclosed by the H-shaped actuation metal. A problem that might occur during the operation of this device is the partial contact with only one contact metal on the handle wafer. In this case no contact resistance measurements can be made.

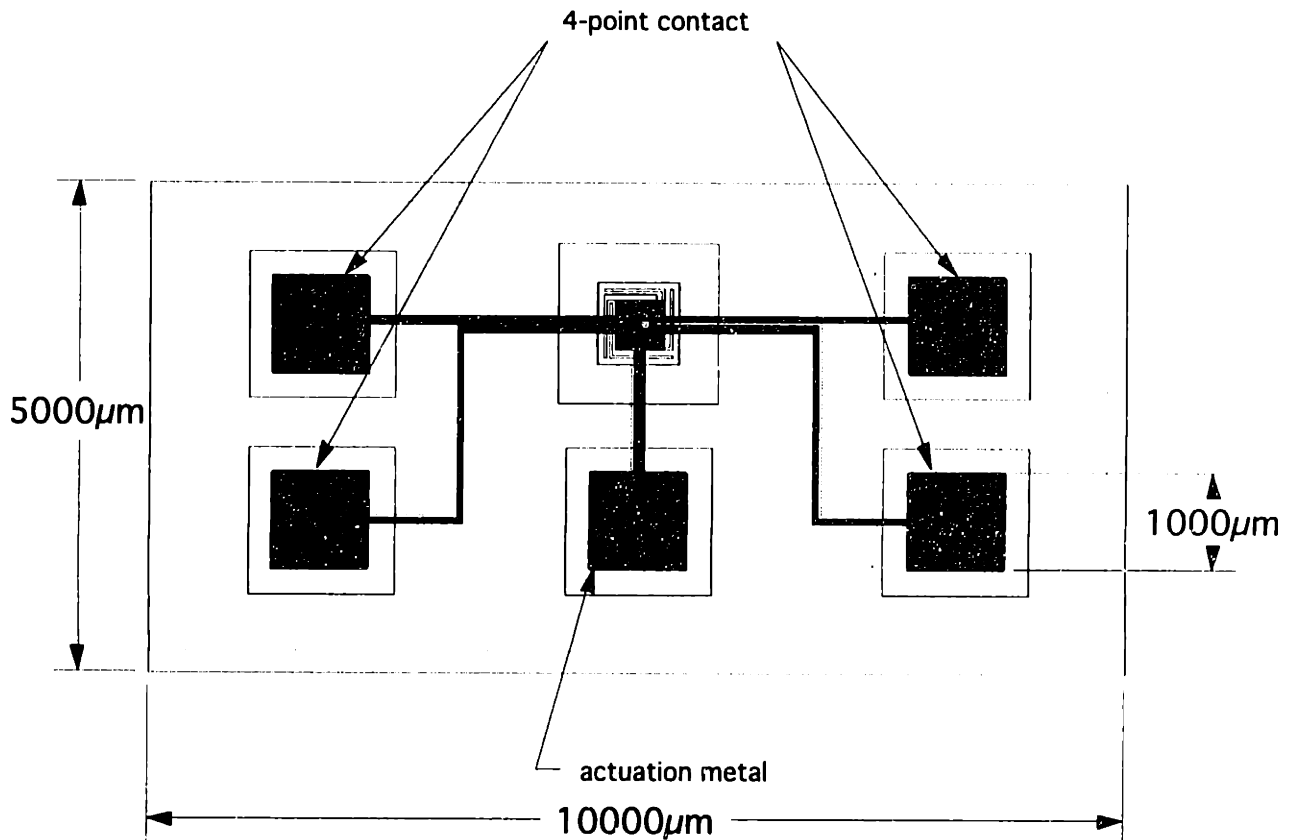


**Figure 2.3.2: Top View of the 4-Point Probe**

In addition to the standard relay we implement several test structures on the wafer to monitor the characteristics of the silicon during the fabrication.

One of the test structures consists of several beams and cantilever etched in the 5  $\mu\text{m}$  thick membrane. Depending on the residual stress in the silicon due to the heavy boron doping the beams will bend. We expect the beams to bend upward or downward depending on the doping concentration. The cantilevers should buckle if compressive residual stresses occur. Since the buckling requires more stresses for the same deflection we expect this structure to be less useful for visual inspection than the test beams.

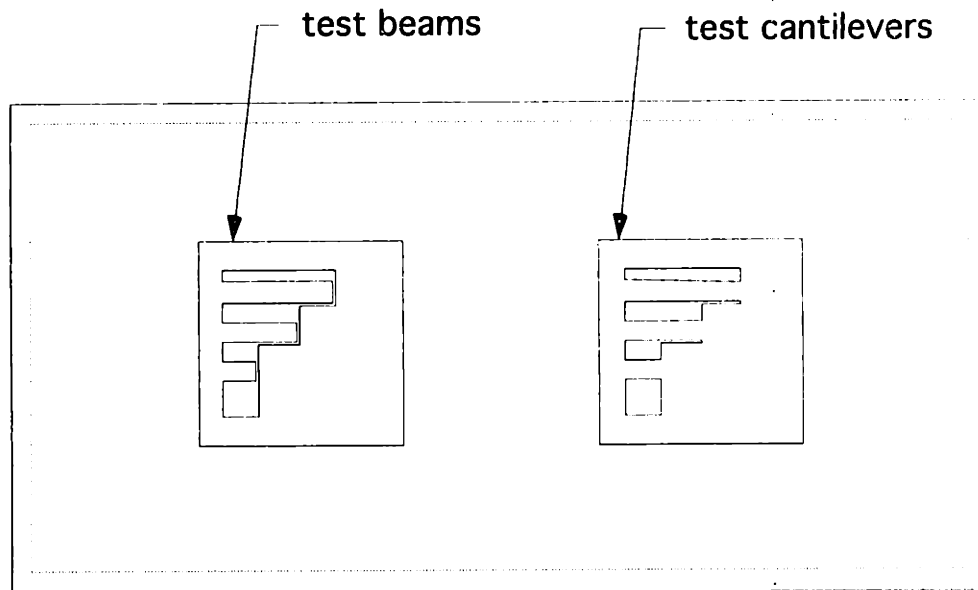


**Figure 2.3.3: Cantilever and Beam Test Structure**



Another test structure that serves a similar purpose as the previous one is shown in Figure 2.3.4. It consists of membranes in different sizes. Again, the residual stress in the boron doped layer cause the membrane to distort.

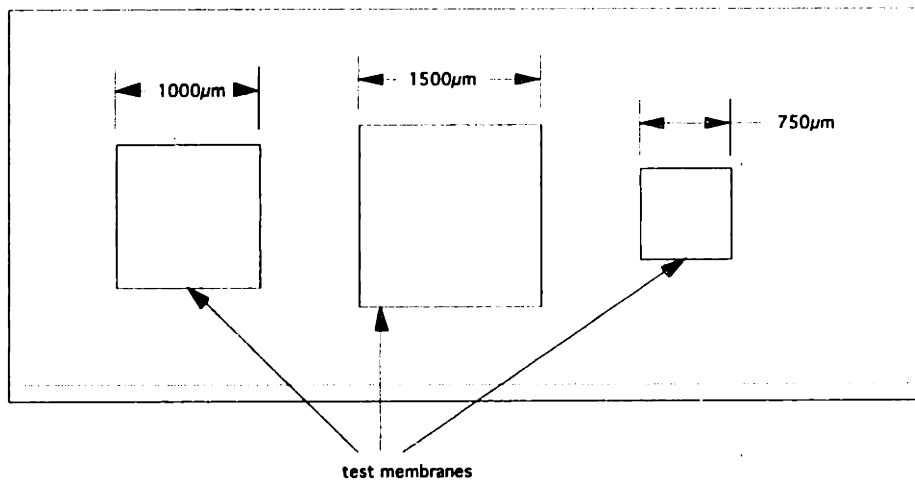


**Figure 2.3.4: Membrane Test Structure**

The third test structure has the three spring sizes on one die. We intend to use this structure to observe the initial deflection of the springs and to perform destructive testing to obtain precise measurements of the trench size and other important dimensions. It is important to mention that all three test structure work only before the bonding of the two wafers. There does not exist a KOH trench on the handle wafer allowing deflection of all three structures after the bonding.

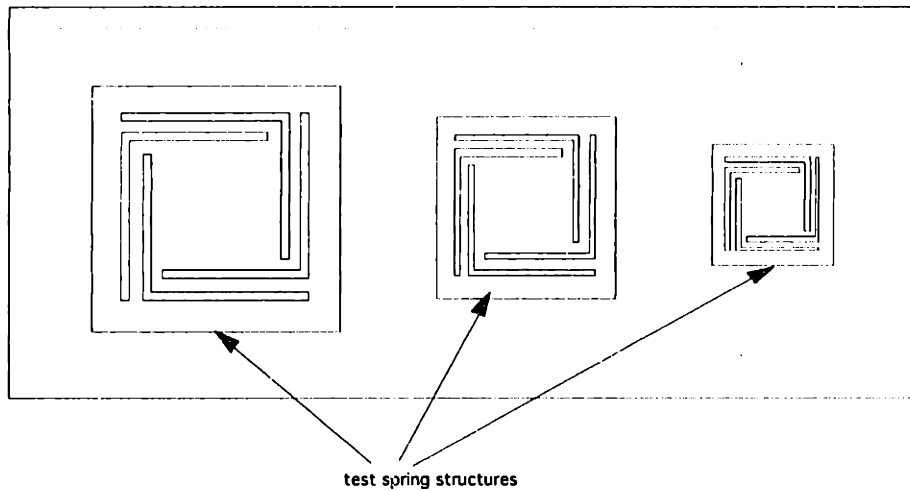


**Figure 2.3.5: Spring Test Structure**

We now describe the mask set for the standard relay. There exists a total of six photolithographic steps for the fabrication of this device. Three steps are required for the spring wafer and three steps for the handle wafer.

The first mask for the spring wafer is a dark field mask that patterns the backside of the spring wafer for an KOH etch. This etch establishes the 5  $\mu\text{m}$  thick membranes for the spring structure and the contact holes. The area of the pattern on the backside of the spring wafer is larger than the desired area of the membranes because of the anisotropic KOH etching. The etch rate in the  $\langle 001 \rangle$  plane is significantly less than in the  $\langle 111 \rangle$  plane. This effect produces trenches that are sloped at an angle of 54.7 degrees as shown in Figure 2.3.6.

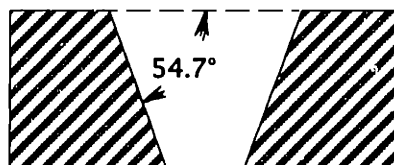


**Figure 2.3.6: KOH Etch Angle**

For example, to produce the membranes for the 1 mm X 1 mm contact holes we need a KOH pattern of 1.2 mm X 1.2 mm.

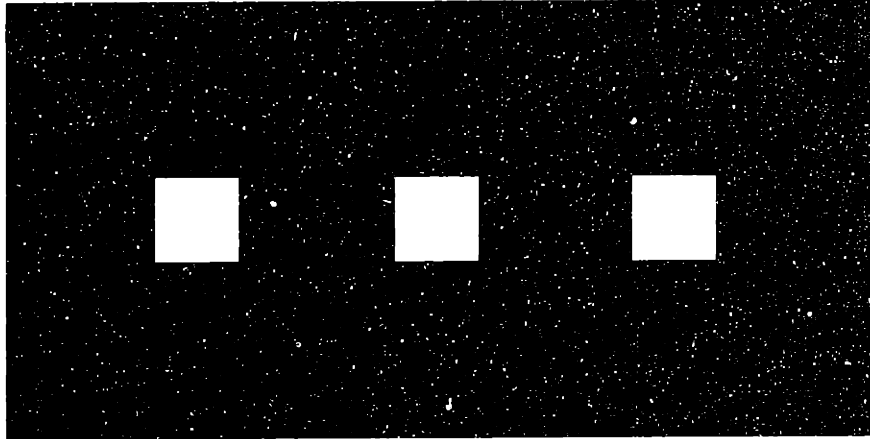


**Figure 2.3.7:** Dark Field Mask for KOH etch on Spring Wafer

The second mask for the spring wafer patterns the contact metal on the front side of the wafer. This is a clear field mask with very few patterns. The biggest problem regarding the patterning of the metal is the alignment of this mask. Since the previous process occurred on the backside of the spring wafer we are unable to pattern any alignment markers on the front side of the wafer. It is therefore necessary to visually align the contact metal to the KOH membranes. The mask is aligned properly if the metal is exactly in the center of the square membrane. Fortunately, the vacuum chuck in the aligner deflects the thin silicon membranes such that we are able to see their location on the front side of the wafer. It is important that we are very precise during the alignment of this mask since the following step depends on its accuracy.

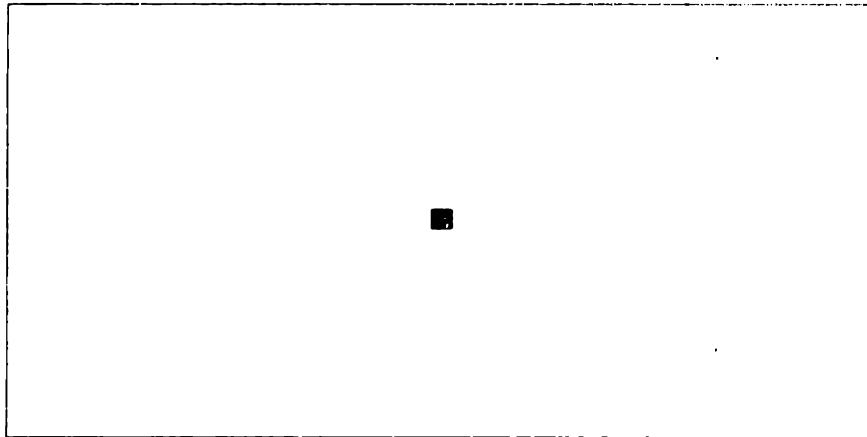


**Figure 2.3.8: Clear Field Mask for Metal Pattern on Spring Wafer**

The final processing step for the spring wafer is the plasma etch that opens the contact holes and relieves the spring structure. The mask for this process is aligned to alignment markers that are patterned with the contact metal mask.

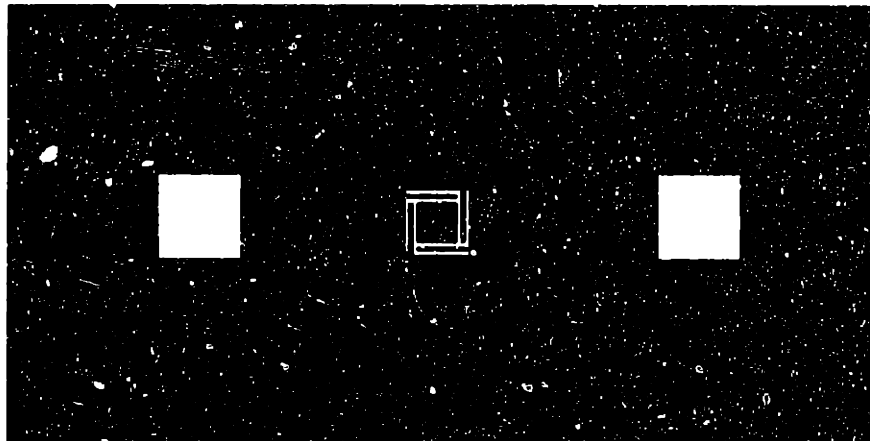


**Figure 2.3.9: Dark Field Mask for Plasma Etch on Spring Wafer**

The first step for the fabrication of the handle wafer is a 5  $\mu\text{m}$  KOH etch to produce a trench for the contact and the actuation metal. The mask for this process is a dark field mask. In addition to the metal trenches we etch a 5  $\mu\text{m}$  deep frame at the etch of the die. The trench is 300 $\mu\text{m}$  wide. It marks the position of each die and prevents shortening of the device after the dicing process. This mask is also used to pattern the photoresist during the bonding process.

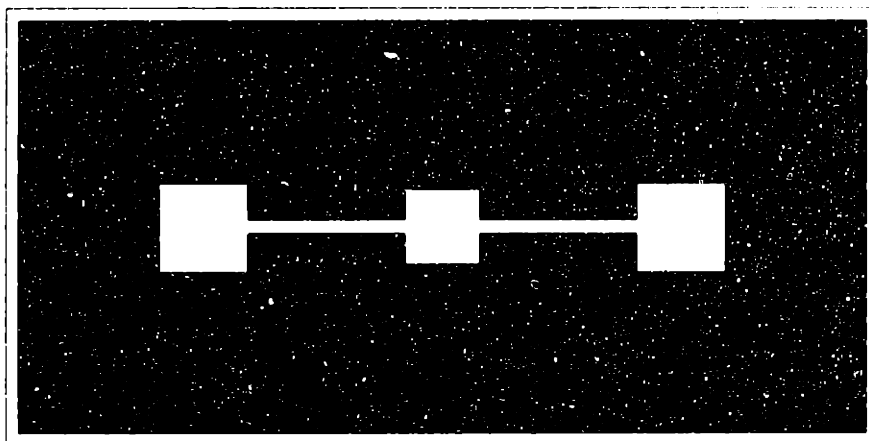


**Figure 2.3.10:** Dark Field Mask for 1. KOH etch on Handle Wafer

The second mask for the handle wafer is similar to the first mask, but it does not feature the 300  $\mu\text{m}$  trench around the edge of the structure. It has a dark square for the contact metal located in the center of the structure. The second 5  $\mu\text{m}$  KOH etch lowers the trench to 10 $\mu\text{m}$  and leaves a square, 5 $\mu\text{m}$  deep pedestal. Consequently, on the pedestal the contact metal is raised 5  $\mu\text{m}$  above the actuation metal.

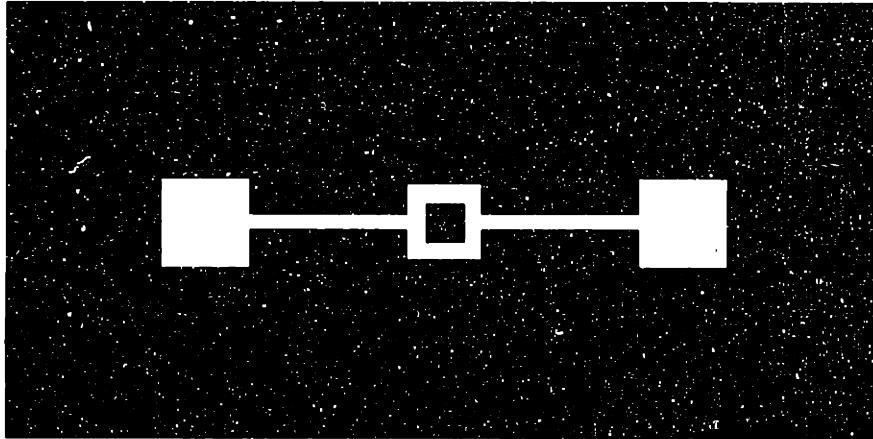


**Figure 2.3.11:** Dark Field Mask for 2. KOH Etch on Handle Wafer

The last mask for the handle wafer is used to pattern the contact and the actuation metal.



**Figure 2.3.12:** Clear Field Mask For Metal Pattern on Handle Wafer

To maximize the yield of all devices on the wafer we position the different structures evenly across the entire area of the 2 inch wafer. To apply photoresist on the spring wafer it must be placed on a vacuum chuck in the spinning station. At the location where the vacuum chuck touches the wafer we cannot have any spring structures since the force of the vacuum will destroy the fragile springs. Consequently, an area of approximately 1 cm<sup>2</sup> in the middle of the wafer cannot be occupied by any structures.

A die size of 5 mm X 10 mm creates 18 available sites for devices on one 2 inch wafer. Since the standard relay is our main priority we divide the die sites in the following way:

3 X 3 sizes of standard relays	=	9
1 X 3 sizes of 4-point probes	=	3
2 x 3 different test structures	=	6

---

Sum	=	18
-----	---	----

The devices are positioned even over the different die sites to maximize the yield of all devices. If one section of the wafer is not functional due to processing failures, there is always a chance that there exist working devices in a different section of the wafer. This can become important if the thickness of the membranes is not uniform across the wafer. Figure 2.3.13 shows a distribution of the die sites.

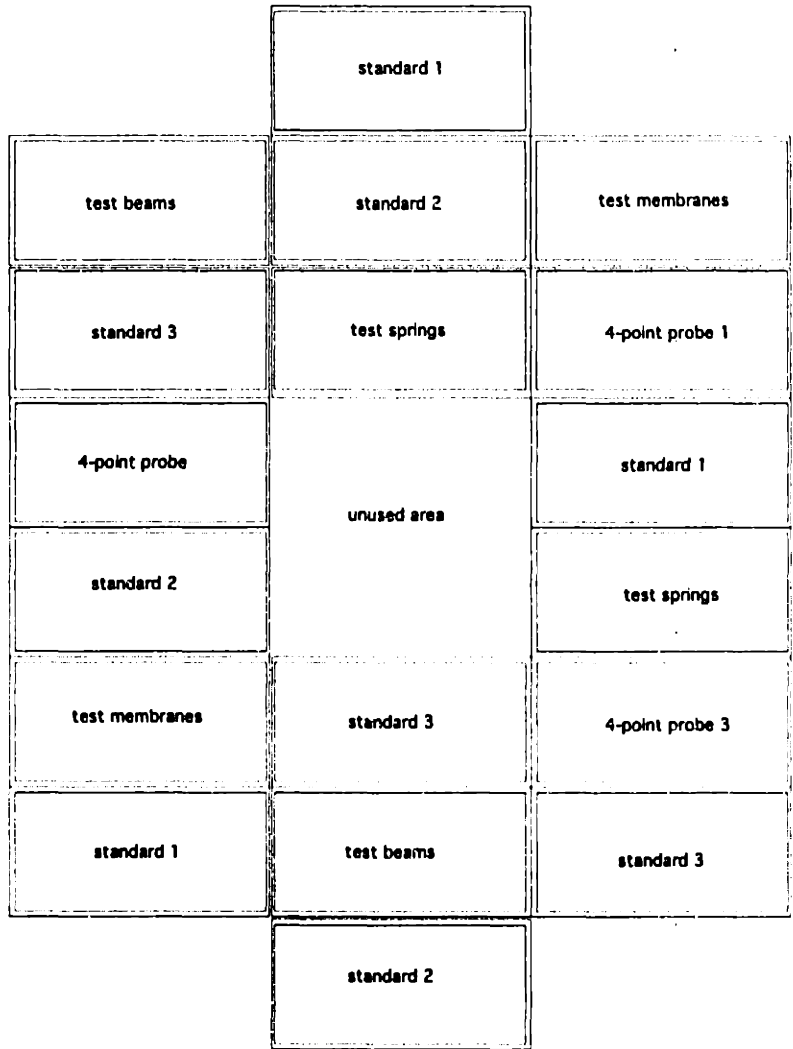


**Figure 2.3.13: Device Distribution**



## **3. Fabrication**

### **3.1. Overview**

The fabrication of prototypes of the micro mechanical relay is accomplished as part of the 6.151J semiconductor project laboratory. The micro relay is the project for the spring term 1994 under the supervision of Professor M. A. Schmidt and Professor C. V. Thompson. In the first half of the course four groups develop the process modules for the different parts of the micro relay. The groups work on the fabrication of the spring wafer, the handle wafer, the metallization, and the bonding and alignment process. In the second half of the course all groups jointly fabricate prototypes of the relay and test them.

### **3.2. Spring Wafer: (as proposed by Testuo Ohara and Remzi Dokmeci)**

For both the spring wafer and the handle wafer we use 2 inch  $p^+$  doped silicon wafers that are polished on one side. The process sequence for the handle wafer starts with the required RCA clean to remove residual organic contaminants. To form the 5  $\mu\text{m}$  thin membrane on the spring wafer we intend to do a KOH etch to a heavily Boron doped 5  $\mu\text{m}$  etch stop. To protect one side of the wafer from the Boron diffusion we first grow a thick layer of silicon dioxide. The oxide is formed by a 10 minute dry oxidation at 1100 °C and a 6 hour wet oxidation at 1100 °C.

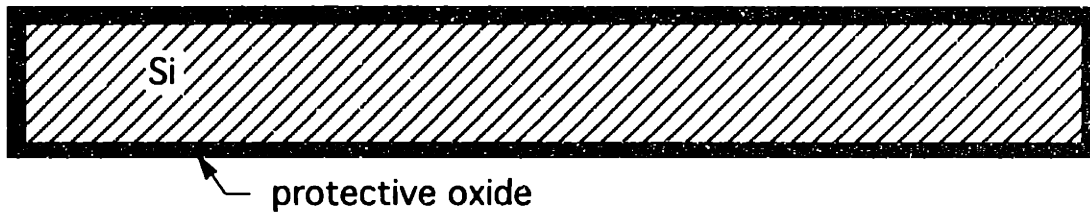


**Figure 3.2.1: Spring Wafer after Oxide Growth**

Now, the oxide must be removed from one side of the wafer. We spin photoresist on the backside of the spring wafer and hardbake it at 135 °C for 25 minutes. A BOE etch for 30 minutes is used to strip the oxide layer on the front side of the wafer. Before we start the boron diffusion we oxidize the boron source for 30 minutes in oxygen at 1150 °C and for 30 minutes in nitrogen at 1150 °C.

In the diffusion furnace the boron is then predeposited on the wafer for 3 hours at 1150 °C. The predeposition occurs in a 10% oxygen ambient. The following drive-in steps take place for 5 hours at 1150 °C in a nitrogen ambient, 1.5 hours at 1150 °C in a dry oxygen ambient and 1 hour at 1100 °C in a wet oxygen ambient.

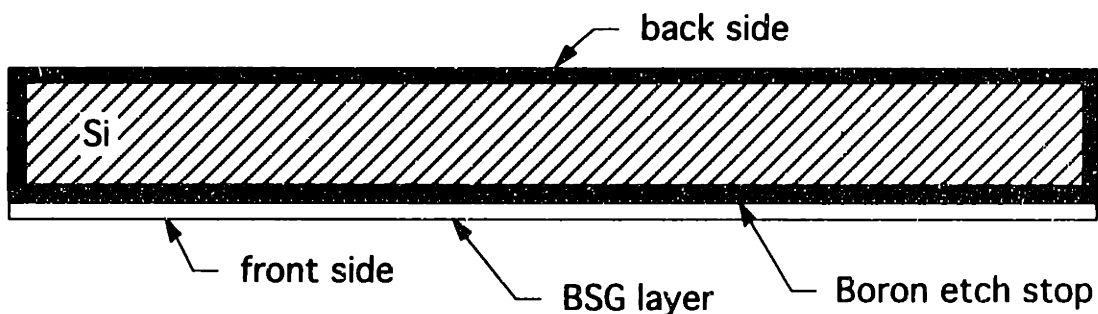


**Figure 3.2.2: Spring Wafer after Diffusion**

The backside of the spring wafer is then patterned with the mask for the KOH etch. The patterned oxide is etched for 40 minute in BOE to create an oxide etch mask for the following KOH etch. The KOH etch is performed in a prepared bath and requires 4 hours of etching at 80 °C. During the etch, the front side of the wafer is protected by the BSG layer that remained after the Boron diffusion.



**Figure 3.2.3: Spring Wafer after KOH etch**

We then remove the BSG and the oxide from the wafer. The next step is the metallization of the spring wafer. The details about a metallization process are prepared by a different subgroup and are described in subsection 3.4.

The deposited metal is then patterned with the mask for the spring wafer contact metals and etched. A problem during the processing is the backside alignment of the contact patterns to the KOH holes. Fortunately, the stress in the doped boron layer and the vacuum chuck in the aligner station cause the silicon membranes to bend, showing the shape of the KOH holes on the front side of the wafer. During the alignment the metal pattern has to be centered to the square KOH membranes.

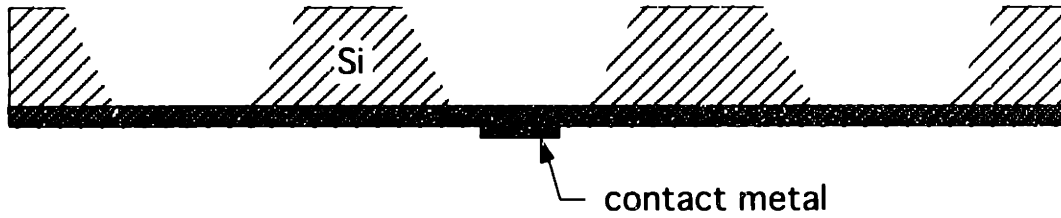


**Figure 3.2.4: Spring Wafer after Metallization**

After the metal has been etched and sintered at 400 °C we align and pattern the mask for the plasma etch to the front side of the spring wafer. Alignment is now easier because we can use deposited metal alignment markers. To open the contact holes and to relieve the spring structure we plasma etch through the 5 μm thick silicon membrane. As parameters for the plasma etch we use a power of 300 Watts, a pressure of 120 mTorr, and an etch time of 3.5 min. The last step before the completion of the spring wafer is the stripping of the remaining photoresist with an organic resist stripper.

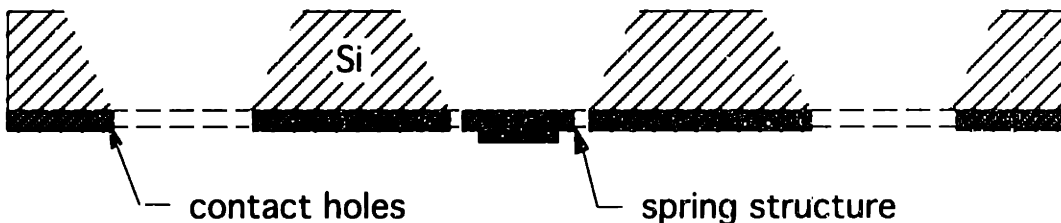


**Figure 3.2.5: Completed Spring Wafer**

### 3.3. Handle Wafer: (as proposed by Laura Juliano)

Like the process for the spring wafer, the handle wafer sequence starts with the required RCA clean.

The main part of the processing for the handle wafer is the KOH etching of two 5  $\mu\text{m}$  trenches that house the actuation and the contact metal. The KOH etch for both trenches uses the same recipe as the spring wafer group with an etch rate of about 1  $\mu\text{m}$  per minute. For the first trench we grow an oxide for the KOH etch mask on the clean handle wafer.



**Figure 3.3.1: Handle Wafer after First Oxidation**

After the oxide has been patterned with the mask for the first KOH trench, we remove the exposed oxide with a 6 minute BOE etch to obtain an etch mask for the KOH etch.

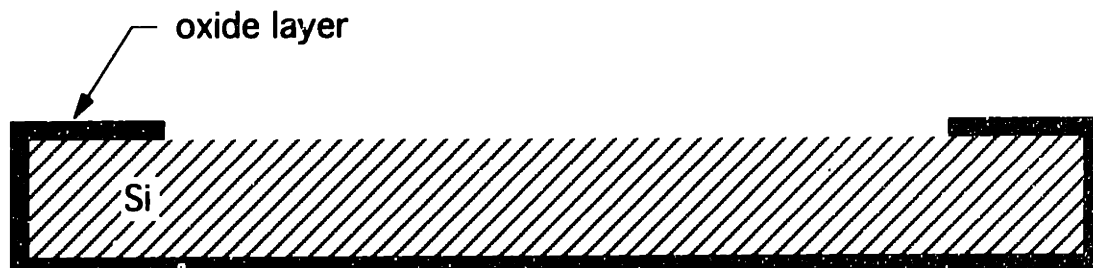


**Figure 3.3.2: Handle Wafer after BOE Etch**

A 5 minute KOH etch will then produce a 5  $\mu\text{m}$  trench.

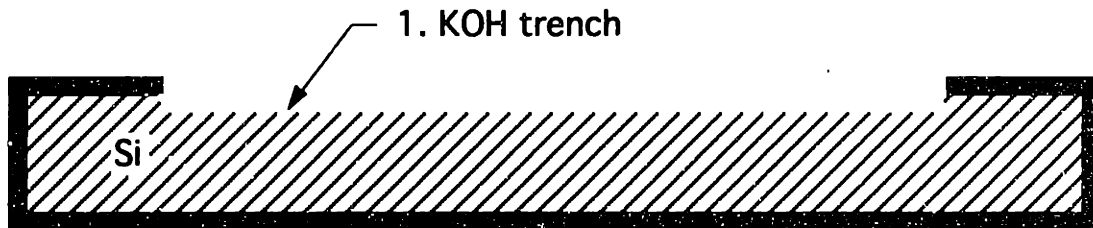


**Figure 3.3.3: Handle Wafer after First KOH Trench**

After another RCA clean we repeat the entire process with the mask for the second trench etch. To avoid any current flow between the contact and the actuation metal we grow an oxide insulation layer on the clean handle wafer. The dry oxidation takes place at a temperature of 1100  $^{\circ}\text{C}$ .

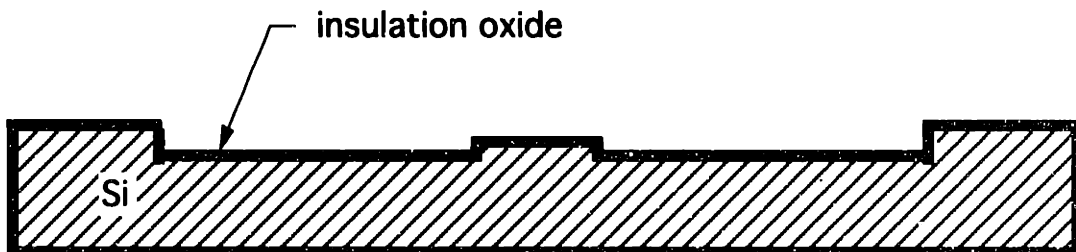


**Figure 3.3.4: Handle Wafer after Oxidation**

The last step of the handle wafer fabrication process is the deposition and the patterning of the metal which is described in Subsection 3.4.

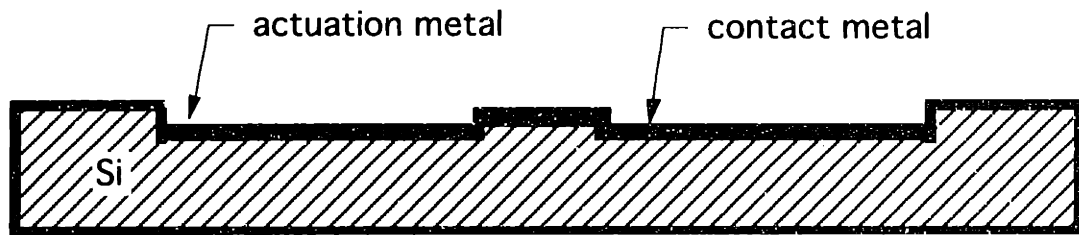


**Figure 3.3.5: Completed Handle Wafer**

### **3.4 Metallization**

A major part of this thesis is the investigation of several contact metals for the micro relay. With the 4-point probe we hope to measure the contact resistance for each metal and select the best material for the relay.

Due to the complicated fabrication process we decide to deposit only aluminum or gold as the contact and actuation metal. For aluminum evaporation, using a resistance heated source is the best deposition technique because it provides a very smooth metal surface and can be easily accomplished in the laboratory. The smooth surface is important for the backside alignment on the spring wafer. The contact metal pattern must be aligned to the shape of the KOH trenches which are only visible on a shiny surface. Consequently, we cannot use sputtering for both the aluminum and the gold deposition because it produces a very rough surface. We deposit the gold using electron beam evaporation.

After the metal is patterned and etched it is important that we use an organic PR stripper or a short plasma etch to remove the photoresist because the Piranha will destroy the metal.

### **3.5 Bonding and Alignment:** (as proposed by Mattan Kamon and Hans-Georg Liemke)

Alignment and bonding of the two completed wafers are the final steps of the fabrication of the micro relay. The functionality of this device significantly depends on the accuracy of the alignment and the reliability of the bonding. Even though we designed this device expecting an alignment error of up to 50  $\mu\text{m}$ , great care has to be taken to keep this tolerance. Larger misalignment will decrease the contact area and will also distort the electric field in the electrostatic actuator. The electric field becomes less uniform and pulls one side of the spring base plate more than the other side, tilting the entire structure. Additionally, a weak bond that cannot sustain even small forces will make it difficult to handle the completed device and limit our ability to test the device.

We investigate several bonding processes to find the most practical approach for the fabrication of our first prototypes. Consequently, our bonding technique might only be applicable to prototyping and cannot be used for the commercial production of micro relays.

A first possibility is an anodic bonding technique to fuse the two wafers applying a high voltage between the two wafers. Unfortunately, voltages in the order of 500 Volts will actuate the spring structures and most likely destroy them.

Another approach is to apply an adhesive material to the wafers, align them, and glue both wafers together. The photoresist spinning station in the laboratory offers an excellent method to apply a thin and uniform layer of liquid adhesive to the wafers. However, it is impossible to spin any material on the spring wafer because the material will flow through the spring structures and the rotational forces will destroy them. For the spin-on material we have the option of using



regular photoresist or polyimide. After testing both materials we decide to use the photoresist because of its improved initial stickiness. This also simplifies the fabrication of the device, because the application and the patterning of the photoresist are standard processes and do not require any special preparation.

To bond the two wafers we dehydrate both for at least 30 minutes in the dehydration bake. We then spin a  $1\mu\text{m}$  thick layer of photoresist on the handle wafer and softbake the wafer for not more than 1.5 min. The short softbake maintains the initial stickiness of the photoresist. After we pattern, expose, and develop the wafer with the mask for the first KOH trench we carefully dry it. Any remaining water droplets on the backside of the handle wafer will cause it to stick to the aligning station.

To facilitate the alignment process we build a customized aligner plate for the Karl Suss aligner (see the machine drawing in appendix A). This plate replaces the mask plate and holds the spring wafer above the handle wafer (see Figure 3.4.1 for details). The vacuum on the aligner plate is only applied around the edge of the spring wafer to prevent the destruction of the spring structures. To align the two wafers we look through the contact holes on the spring wafers and position them to the metal on the handle wafer. With the Karl Suss aligner the wafers can be precisely positioned. Just before we bring the two wafers into contact we apply a small drop of water to the edge of the handle wafer. The surface tension of the water will provide the initial adhesion that is required to handle the two aligned wafers.

The device is then sandwiched between two aluminum cylinders, placed on a hot plate and heated to  $300\text{ }^{\circ}\text{C}$ . The ends of the cylinders have a flat surface to provide uniform pressure across the area of the wafer. The bonding of the wafers is completed after 30 minutes of this simultaneous pressure and heat application. Unfortunately, the photoresist bond is not permanent and

deteriorates over time which prohibits the use of this method in the production of commercial relays. Usually the bond does not last longer than a week. For permanent bonding of the device it is therefore necessary to apply small amounts of epoxy at the edge of the wafer. Bonding at the edge is sufficient since we do not consider dicing during the preliminary testing of the device. Figure 3.4.2 shows a cross section of the completed relay.

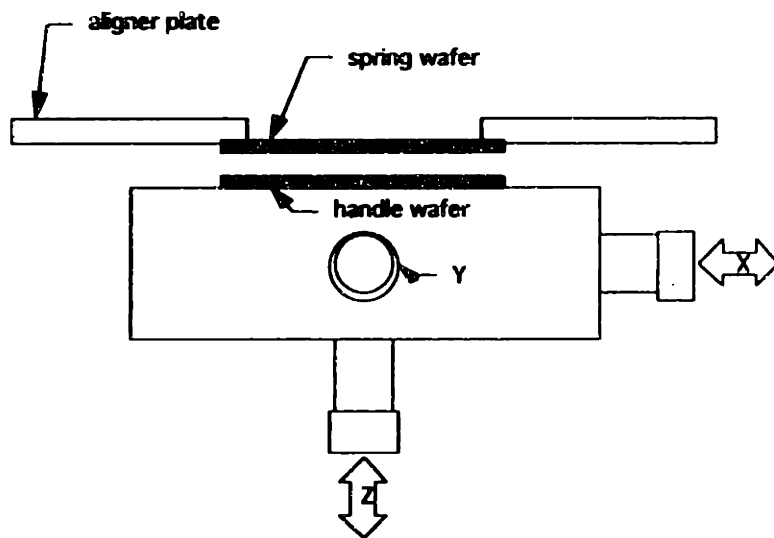


**Figure 3.4.1: Alignment Station**



**Figure 3.4.2: Completed Micro Relay**

## **4. Results**

### **4.1 Fabrication Results**

We did not experience any major complications during the fabrication of this device and were able to finish the individual process modules within our planned schedule. Minor problems concerned the thickness of the KOH membranes. It seems that we used depleted Boron sources in the end of the processing. Consequently, there was a gradient in the doping concentration across the wafer and the following KOH etch produced a non uniform membrane thickness. During the following plasma etch we were unable to etch all structures on the wafer uniformly. In order to produce working structures some springs had to be destroyed by over or under etching.

It also occurred once that we accidentally sintered the metal after the plasma etch. It was interesting to observe how thermal stresses induced by the high temperature sintering process (400 °C) deformed the spring structures and made the actuation of these structures impossible.

Figures 4.1.1-4.1.3 show SEM pictures of the completed spring wafer and the completed handle wafer.

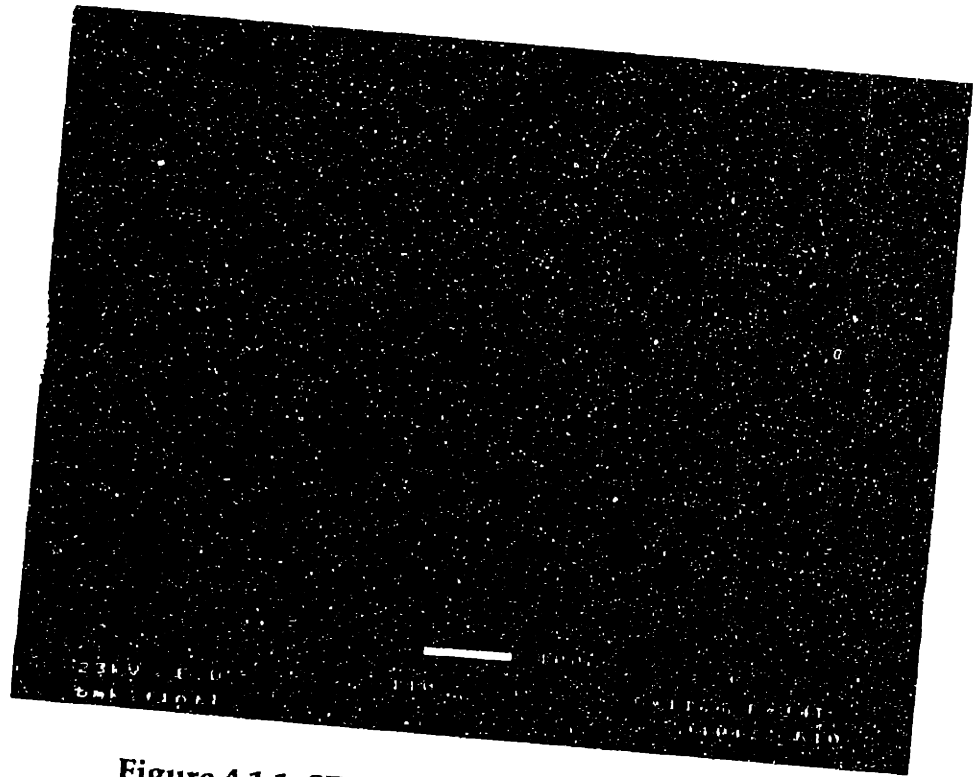


**Figure 4.1.1: SEM Picture of Spring Structure**

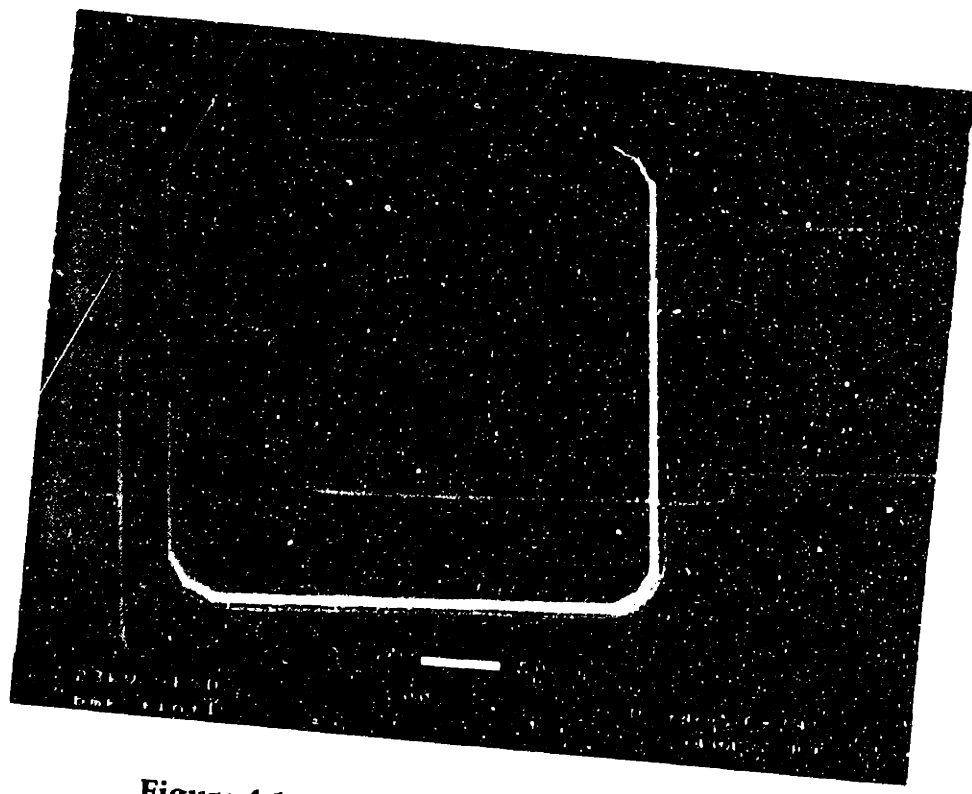


**Figure 4.1.2: SEM Picture of Contact Metal**

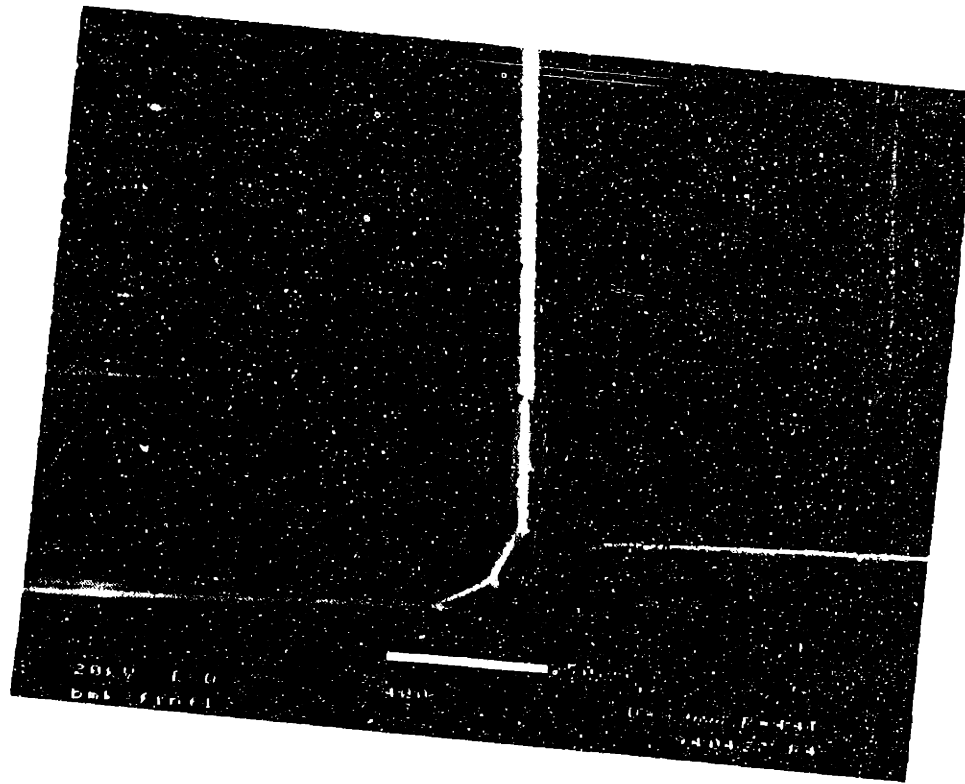


**Figure 4.1.3: Magnified View of Contact Metal**

Figure 4.1.1 shows the etched spring structure and a slight shadow of the contact metal on the spring base plate. Figure 4.1.2 and 4.1.3 show the KOH trenches with the actuation and contact metal on the handle wafer. Looking at Figures 4.1.2 and 4.1.3 it occurs that there is a small ring of remaining contact metal around the etched pedestal. In the magnified view in Figure 4.1.3 we can see that the separation between the contact and the actuation metal at this point is only 10  $\mu\text{m}$ . There exists the possibility that some devices are not functional if there is a connection between both metals. A reason for the metal ring is probably remaining photoresist that is not removed by the developer.

## 4.2 Experimental Testing Results

Several important observations were made during the preliminary testing of the first relay prototypes.

The test structures were examined before the bonding of the two wafers. Under the microscope we could see little deflection of the spring and membrane test structures. However, by eye inspection it seemed that the membranes were bending upward (bending above the surface of the spring wafer front side). The beam test structure deflected upward due to the stress distribution in the 5  $\mu\text{m}$  membranes. The upward deflection suggests that a high boron concentration causes compressive stress. The highly doped wafer surface contracts more than the deeper regions and bends the 5  $\mu\text{m}$  membrane. As predicted, the longest beams showed the largest deflection and we were able to approximate their deflection by changing the focus of the microscope. It was found to be around 25  $\mu\text{m}$ , but this measurement is very subjective and depends on the focus point of the observer. The cantilevers showed no bending or buckling, probably because the magnitude of the residual stress was not sufficient for a visible deflection.

During the testing of the very first prototypes which were primarily aluminum devices we observed a poor yield of the spring structures. Most of the springs, generally the larger, less stiff structures were destroyed during the processing. Additionally, a large number of springs were deformed and stuck to the metal on the handle wafer. The structures were touching both the contact and the actuation metal and it seems that the large current fused the spring structure to the actuation metal. However, we also observed that at some structures current was only flowing between the actuation metal and the spring wafer. This

means that the base plate tilted as shown in Figure 4.2.1, or that after the bonding some photoresist remained on the pedestal and insulated the contact.

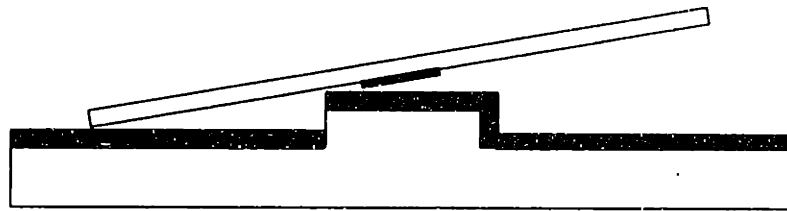


**Figure 4.2.1: Tilted Spring Structure**

Yet, Some of the structures were not initially stuck and we were able to actuate them at various voltages between 20 V and 150 V until the spring stuck to the actuation metal after the first pull down and would not return to their original position. During the actuation one could see a color change of the structure indicating the movement of the base plate.

Further tests with improved wafers that had better springs and gold metal also showed an initial actuation of the spring until it stuck to the handle wafer. Here, the large springs pulled down between 35 V and 70 V, the medium springs around 100 V, and the small springs around 100 V. However, we now decided to touch the base plate of the spring with a probe tip and pull the structure back up. Repeating this test several times we found the results to be repeatable with the actuation voltage being within a range of about 20 V. For a few cycles some structures showed continuous actuation and returned to their original position after the actuation voltage was turned off. In this case the observed color change of the structure was not uniform and we assume that the structure was not pulled down vertically and tilted as shown in Figure 4.2.1.

Finally, a 4-point probe measurement was made on a relay with gold metal. We used a fifth probe to press the spring on the contact metal because the

structure could not be actuated properly. With this simple approach we measured a contact resistance of  $8.43 \Omega$ .

## 5. Conclusion

Our fabrication process turned out to be fairly reliable and it was simple enough to be accomplished in the 6.151J project laboratory. However, we experienced several problems during the fabrication and the testing of this device that could be improved in future projects. First, the fact that we were unable to predict the residual stresses in the material caused several difficulties. Most structures that were etched in the membranes deflected due to the unpredictable residual stresses. These distortions are the main reason why the springs tend to stick to the handle wafer. To improve this device, we have to find a way to predict the stresses in the material and derive the resulting deflection of the structure. Unfortunately, this is very difficult and requires knowledge of all fabrication parameters as the effect of the sintering after the plasma etch shows (see section 4.1.1).

In some cases we observed that the movement of the springs is not exactly vertical. A reason for the tilting of the base plate might be a gradient in the thickness of the springs or the asymmetric shape of the actuation metal. In future designs it might be advisable to make the actuation metal more symmetrical.

To avoid that the spring sticks to the actuation metal improved design should include additional pedestals that keep the spring base plate from touching the actuation metal. Here, only the masks for the handle wafer have to be slightly modified as shown in Figures 5.1 and 5.2.



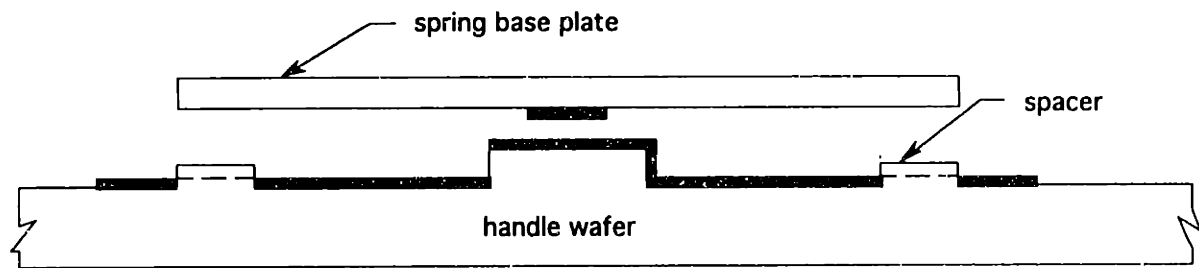


**Figure 5.1: Improved Switch Structure**

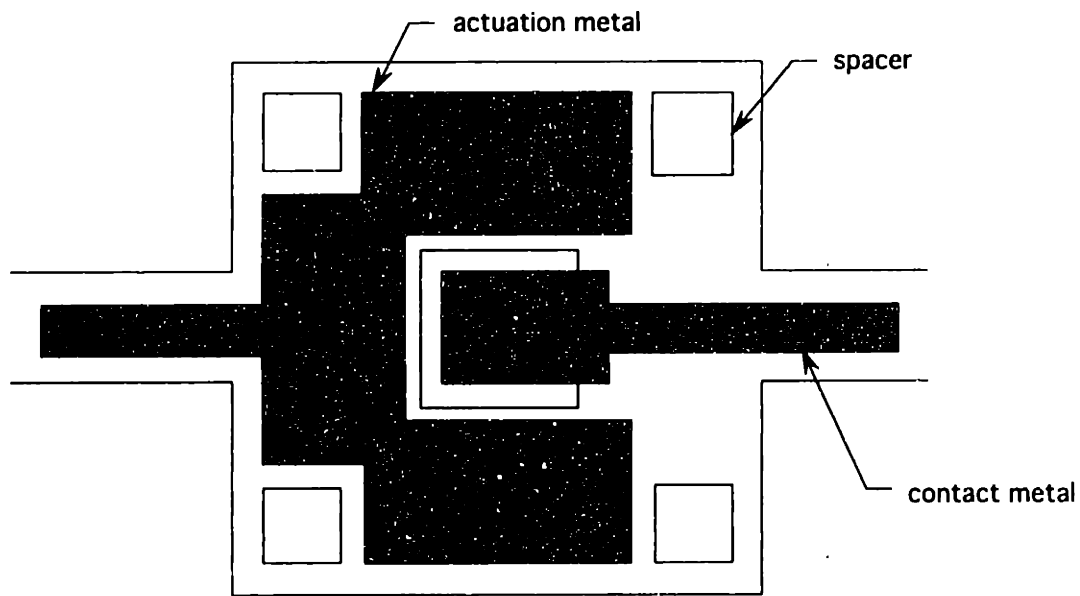


**Figure 5.2: Top View of Improved Handle Wafer**

With our existing mask set it might also be possible to lower the second KOH and increase the gap between the actuation metal and the spring to more than 10  $\mu\text{m}$ . It is possible that we can produce a trench that is deep enough that the spring does not touch the actuation metal and still have a reasonable actuation voltage.

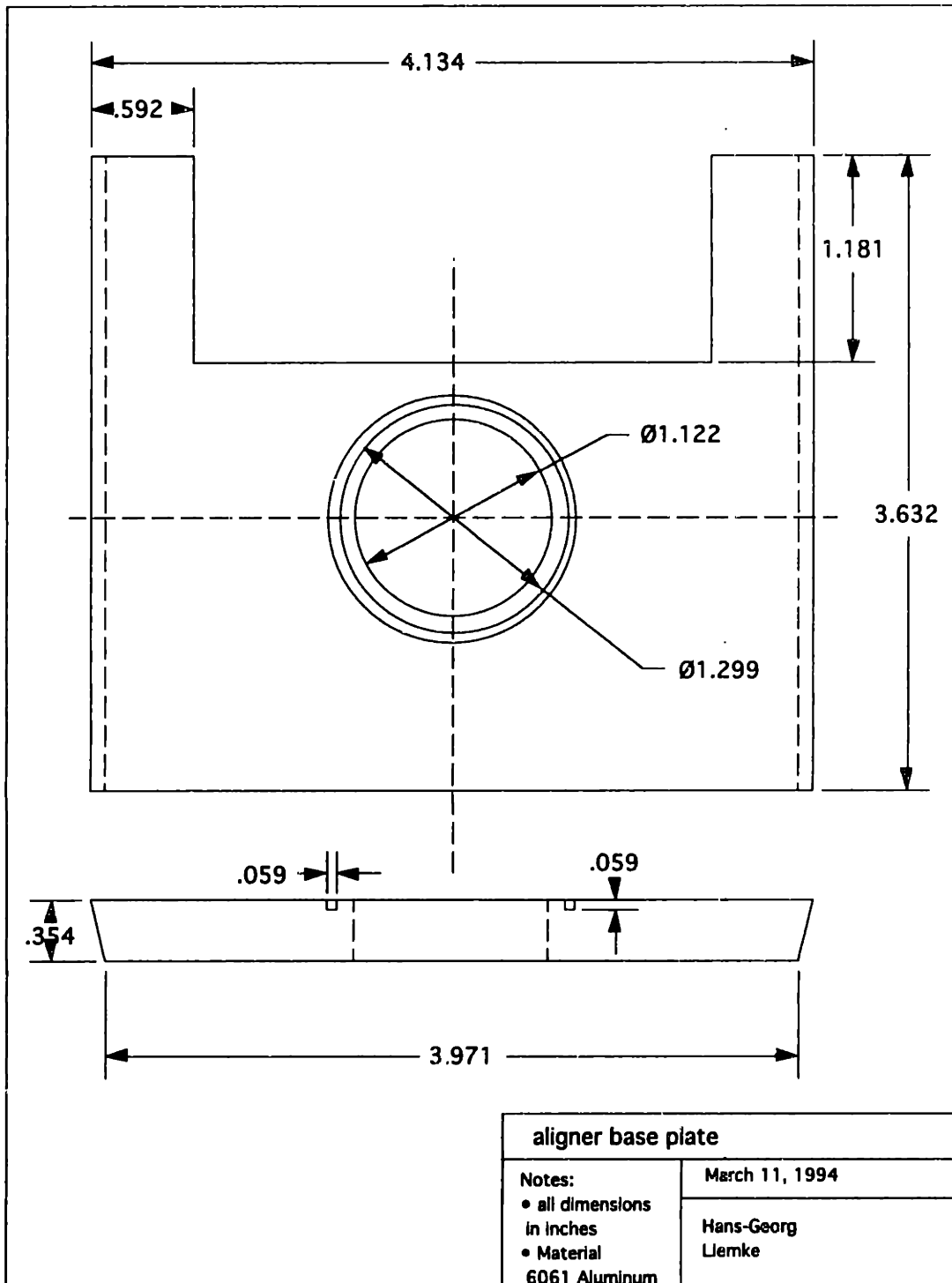
Other things that we should do differently in the future are KOH trenches under the test structures such that we are able to test them after the bonding.

If we manage to produce working devices we can try to reduce the feature size of this structure to the limit of the fabrication equipment. In this case we have to be very careful with the alignment and the bonding of the wafers.

Additionally, it can be useful to simulate the performance of the relay using MEMCAD simulation software even though this task will be very time consuming and difficult. On the other hand, it will give us a better understanding of the dynamics of this system.

Further investigation can also address the natural frequency of the structure and its frequency response.

# Appendix A



# Bibliography

[1] Hosaka, Kuwano, and Yanagisawa. Electromagnetic Microrelays: Concepts and Fundamental Characteristics. In proceedings, Micro Electro Mechanical systems, pages 12-17. IEEE, 1993.

[2] Mitchell J. Novack. Design and Fabrication of a Thin Film Micromachined Accelerometer. M.S. thesis. Mechanical Engineering MIT, 1992.

[3] S. Wolf and R.N. Tauber. Silicon Processing for the VLSI Era, page 647. Lattice Press, 1986.